

THE LASER SIGNATURE IN CALIBRATION OF THE SERVOMECHANISM

Edward F. Plinski*, Antoni Izworski**, Jerzy S. Witkowski*

*Institute of Telecommunications and Acoustics, Wrocław University of Technology,
Wybrzeże Wyspińskiego 27, 50-370 Wrocław, Poland

**Institute of Engineering Cybernetics, Wrocław University of Technology,
Wybrzeże Wyspińskiego 27, 50-370 Wrocław, Poland

Keywords: Servo-mechanism, process automation, CO₂ laser, laser signature, adaptive system, expert system

Abstract: The laser signature, which can be observed as a result of the CO₂ laser tuning, is used as a standard for calibration of the servomechanism. The servomechanism can be used for continuous investigations of the laser signatures of different laser media. Finally, some convenient signatures useful for a laser marker or single frequency laser operation can be found.

1 INTRODUCTION

When we consider the optical device called a laser, than we can recognize two “sets” of frequencies produced in the device: a set of emission line frequencies ν_L of the excited laser medium (or a singular line, which takes part in laser operation), and a set frequencies ν_R possible to obtain in an optical resonator – see Figure 1.

When the laser is tuned (Figure 2), then the laser longitudinal mode, let us say ν_{q+1} , restores the profile of the emission line giving a laser output gain curve – see Figure 1. The gain curve is observed with each half-lengthwave $\lambda/2$ tuning ΔL (from a node to node of the standing wave in the resonator cavity), where L – length of the optical resonator. The resonator tuning is indicated in Figure 1 with the arrow. Bottom figure – the laser gain curve obtained when the laser is tuned of half-lengthwave (ΔL – a translation of the laser mirror M_R).

The picture is much more complicated, when the excited laser medium creates many emission lines. The CO₂ medium is a good example – see a model of the laser signature given in Figure 3. A line hoppings effect is observed (Mocker, 1968).

A spectrum of the CO₂ molecule consists a number of emission lines grouped in many bands, and branches.

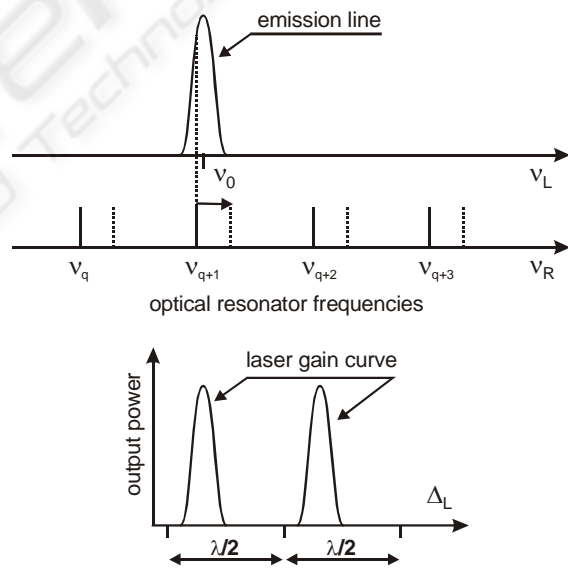


Figure 1: Mechanism of the laser generation (a model) on frequency ν_{q+1} in the range of the emission line with a center at ν_0 . (ν_R - frequencies of the laser medium spectrum, ν_L – resonant frequencies of the optical resonator (longitudinal modes)).

The most useful for the CO₂ laser operation is a band with the frequency center of appr. 10.4 μm . The band consists of two branches P, and R, where the strongest line P20 is the most attractive for the

laser operation – (Wittman, 1987). When we tune the laser resonator, then different resonant frequencies (longitudinal modes) of the optical resonator can be in coincidence with frequencies of the emission lines of CO₂ laser medium.

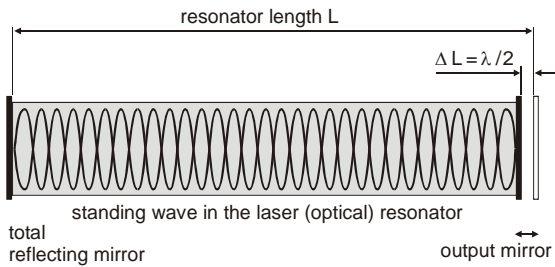


Figure 2: The rough scheme of the laser. The laser can be tuned with a piezo-ceramic transducer (see output mirror) of a few values of the half-wave ΔL .

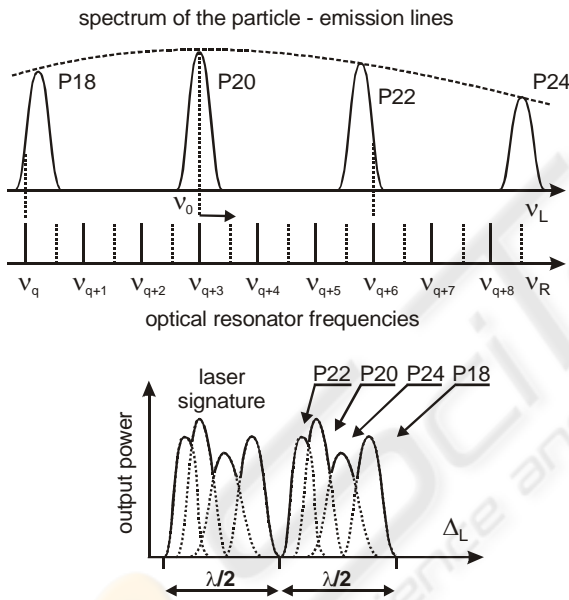


Figure 3: The laser signature developing (a model), when the laser resonator is tuned of a half-wavelength (from a node to node). The names of the emission lines are indicated (top). The line hoppings effect is shown (bottom) during the signature developing.

Of course, each line being in coincidence with the resonant can take part in laser action. Theoretically, the laser can operate on many emission lines simultaneously. Fortunately for the experiment, a strong competition exists between different rotational levels in the CO₂ medium, and the laser usually operates only on one chosen line, as a consequence (Mocker, 1968). Exactly, on that line, which center frequency ν_0 is the closest to the

resonant frequency ν_q of the resonator. Figure 3 explains the effect. As seen, the resonant frequency ν_{q+3} is the closest to the center of the emission line P20. When the resonator is tuned, then we can expect “jumps” from line to line (a line hoppings effect). The observed picture of the output laser power is called a laser signature (Waksberg, 1971). The signature is reproducible with each half-lengthwave $\lambda/2$ of the tuning ΔL (usually a few signatures – a few $\lambda/2$). The laser signature is stable, and easy to calculate for the chosen length L of the optical resonator – see Figure 2 (Shiffner, 1972).

2 EXPERIMENTAL

The RF excited laser shown in Figure 4 is equipped with aluminium electrodes with an area 380 x 20 mm² (top), and 400 x 110 mm² (bottom), spaced by 2 mm. The laser head is fed with an RF generator of 2kW power via a matching circuit (Plinski¹, 2000). The negative branch unstable resonator consists of a rear mirror M_R with a radius of 430 mm and output mirror M_O with a radius of 370 mm.

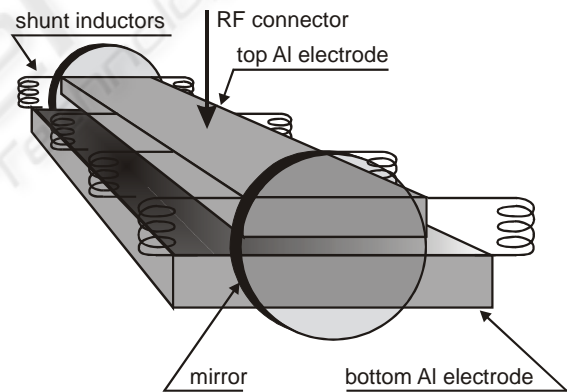


Figure 4: Scheme of the slab-waveguide laser structure.

The mirror spacing, defined by a low expansion Invar bar, is $L = 402$ mm in length for appr. confocal operation, but it can be increased to 414 mm giving a diverging output beam. The rear mirror M_R mount is fixed to a piezo-electric transducers (PZT), for cavity length scanning (a few wavelengths). The positive branch unstable resonator with a rear mirror $M_R = 5800$ mm and an output mirror $M_O = 5000$ mm, giving a geometrical out-coupling of 16%, creates the second structure of the laser used in the experiment. Figure 5 shows a real result of the investigations on the laser signatures. The laser is tuned of $\Delta L = \lambda/2$. The signal is registered with a

HgCdTe detector, and a scope (compare to Figure 3). When the laser is tuned we observe a line hoppings effect.

A similar experiment is performed with the laser equipped with a positive branch unstable resonator. The result is shown in Figure 6. It presents a partly well-ordered signature (WOLS effect, Plinski², 2000), where P lines are splitted up by a few lines of an R branch (10.6 μm band) – exactly, the lines appear in the order: P24, R14, P22, P20, R18, P18, P16, R16, P14.

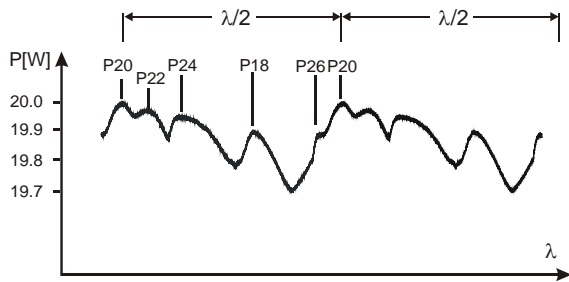


Figure 5: The laser signature. Changes of the laser output power with tuning (translation) the laser mirror (see Figure 2).

The result is obtained on a 414 mm long optical resonator. A diffraction grating is used to recognize the CO₂ laser emission lines. The output laser beam is deflected at the grating into different angles and visualized at the UV screen (top).

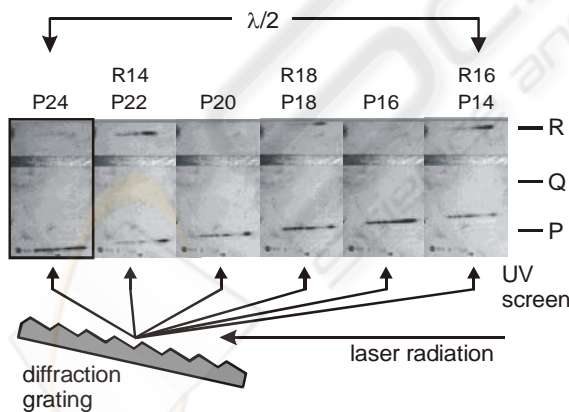


Figure 6: Partly well-ordered signature (P lines) obtained on a positive branch unstable resonator of the slab-waveguide CO₂ laser. The pattern of the output laser beam is visualized at the UV plate.

We elaborated a numerical procedure, which calculates the laser signature for given frequencies of the emission lines, and given length *L* of the optical resonator (the shape of the emission lines is

not taken into account) – see an example of the calculations in Figure 7.

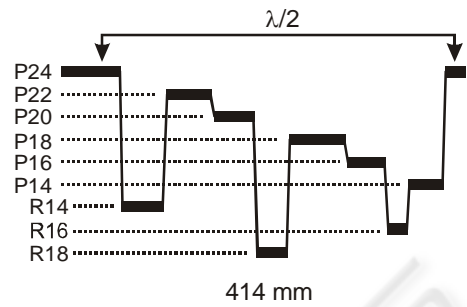


Figure 7: Graphical representation of the laser signature from Figure 6, calculated theoretically.

The series of signatures in line creates a specific picture (histogram) of the carbon dioxide laser for some strictly determined spectrum of the laser medium.

3 AUTOMATION OF THE INVESTIGATION PROCESS

The automatic control system consists a set of piezoceramic transducers (PZT), and a micrometric screw MS with a motor-driver MD. The process of the calibration is done in four steps (see Figure 8):

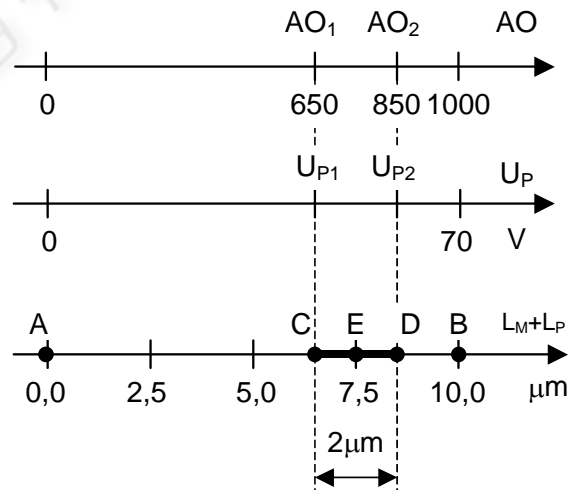


Figure 8: Mutual relations between *AO* control signal on the step motor, *U_p* voltage on the piezoceramic transducer PZT, and translation of the mirror *L_M+L_P* (*L_M* – initial position of the mirror, *L_P* – final position).

- 1-st step: voltage from 0 to 70 V on PZT with 0,1V resolution – the signature is recorded;

- II-nd step: jump from 70 to 0 V on PZT (move back);
- III-rd step: 3 steps of the motor (move forward, appr. $3 \times 2,5 \mu\text{m}$) to „hit” the section CD;
- IVth step: correction voltage on a PZT to „hit” the signature obtained in the I-st step.

1 - transducers PZT tune the laser resonator (translates the mirror M_R) of a few $\lambda/2$ (it depends on the kind of the PZT) – a lower trace,
 2 - the PZT comes back to the same position (the same length L of the resonator) – the 2 voltage on the PZT is set on the initial value – a medium trace,
 3 - the screw MS takes over the role of the translator; the screw translates the laser mirror of the same distance (a few $\lambda/2$) with suitable corrections using PZT – a upper trace,
 4 - the PZT takes over the role of the translator again (see Figure 9)

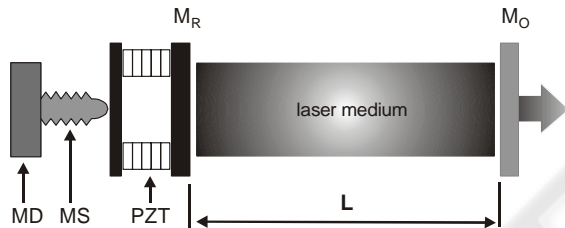


Figure 9: The scheme of the laser used in the experiment. The laser can be tuned with a motor-driver MD equipped with a micrometric screw MS, and piezo-ceramic transducers PZT of a few values of the half-wave ΔL . M_R – rear, total reflective mirror, M_O – output mirror.

3.1 Details of the automation – intensity recognition

The algorithm of the control of the calibration process is given in Figure 10. The control object under investigation is controlled by tuning the micrometric screw MS to obtain the screw travel of L_M . The screw travel is equal to $\Delta L_M = 500 \mu\text{m}$ per one turn, and the total operating length equals $L_{M \max} = 20 \text{ mm}$. (Only part of the operating length is used in the experiment: $L_M \in [0 ; L_m]$, where $L_m < L_{M \max}$). The screw is operated by a stepped motor enabling to make 200 steps per one complete revolution of the motor. Thus, an expected screw linear travelling is equal to $\Delta L_M = 2.5 \mu\text{m}$ per one revolution of the motor (Plinski², 2003).

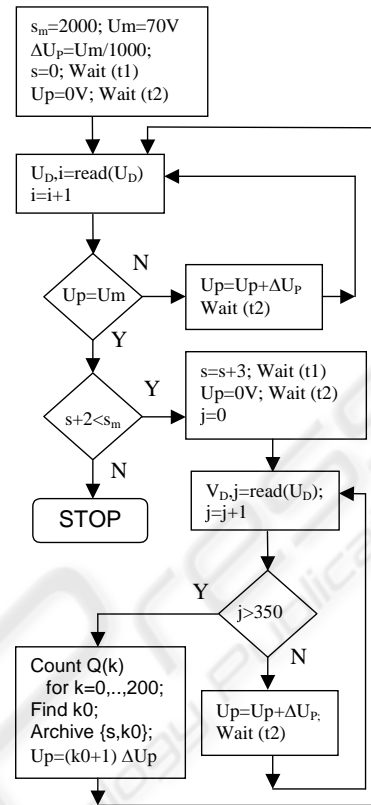


Figure 10: Algorithm of the calibration process.

Another actuating track is a piezoceramic transducer (PZT) that enables to achieve the shift within the range of $L_p \in [0 \div 10 \mu\text{m}]$ for the input voltage $U_p \in [0 \div 70 \text{ V}]$. As shown above, comparing the operating ranges of the step motor and piezoceramic transducer, 4 steps of the motor correspond to the control range that is obtained by voltage changes U_p from 0 V to $U_m = 70 \text{ V}$. The informations that the object under control has moved out is obtained due to the HgCdTe detector that provides the informations on the intensity of the laser beam. The time constant of the detector does not exceed one millisecond.

It is recommended solution for the automation processes used in industry (Solnik, 2000), as the control member, the industrial controller SAIA PCD2 is applied. The manual control mode and monitoring of the current control parameters may be realised with the operator’s terminal. On the other hand, the operator’s station SCADA (Supervisory Control And Data Acquisition) serves, primarily, for creation of the experiment archives and for storage of the database. All measuring and actuating tracks are provided with galvanic isolation that decreases the impact of disturbances upon

operation of the system. Also because of the need to decrease the disturbance impacts the experiment results, the current standard has been used for analogue signals.

As a turn with the motor results in the shift value of L_M with a relatively high error of appr. $1 \mu\text{m}$, a voltage correction procedure for the shift is introduced. A real shift $\Delta L_{1R} = 2.5 \mu\text{m} \pm 1 \mu\text{m}$ is introduced for the single step of the motor. The change of the voltage U_p in a full range results in 4 steps of the motor. In the correction procedure: first - the voltage U_p on the PZT is increased up to 70 V; second - the voltage is decreased to 0 V, and 3 steps of the motor are introduced. Then, a resultant shift of the mirror equals $\Delta L_{2R} = 7.5 \mu\text{m} \pm 1 \mu\text{m}$. As an exact position of the mirror is unknown, the operating system looks for the correction voltage U_p resulting in shifting the mirror to the place, which can be reached by an ideal motor. In that way, periodic executions, as above, allow increasing the mirror shift of $3 \times 2.5 \mu\text{m}$ for each cycle (with the resolution of $0.01 \mu\text{m}$).

Expressions (1) and (2) describe the value of the shift L_p versus a signal AO on the transducer C/A and the voltage U_p . Expression (3) gives the value of the shift L_M versus a number s of the motor step.

$$U_p = AO \cdot \frac{U_M}{1000}, \quad AO = 0,1,\dots,1000, \quad U_M = 70V, \quad (1)$$

$$L_p = 10\mu\text{m} \cdot \frac{U_p}{60V}, \quad U_p = 0V,\dots,70V, \quad (2)$$

$$L_M = s \cdot 2.5\mu\text{m}, \quad s = 0,1,\dots, \left[\frac{L_M}{2.5\mu\text{m}} \right]. \quad (3)$$

Measurements of the laser response U_D^i give at least 1000 values, when the L_p is changed in the range as in (2):

$$\{U_D^i\} = U_D^1, U_D^2, \dots, U_D^n; \quad n \geq 1000. \quad (4)$$

After next 3 steps of the motor, and putting $U_p = 0$ V on the PZT, the U_p voltage can be increased according to (1) giving a sequence of values $AO = 0,1,\dots,350$ on the transducer.

$$\{V_D^i\} = V_D^1, V_D^2, \dots, V_D^{350}. \quad (5)$$

At least 151 responses V_D^i is taken from the measurement range (4). The goal of the operation

system is to determine the index k of the response V_D^k , which corresponds to the voltage U_D^{n-250} (for the ideal step motor, and micrometric screw $k = 0$).

Expression below describes an assumed quality function (classic one used in identifying processes, and approximation quality evaluations):

$$Q(k) = \sum (U_d^{750+j} - V_D^{j+k})^2, \quad k = 0,\dots,200. \quad (6)$$

The minimum value k_0 is assumed to minimize the functional $Q(k)$:

$$Q(k) = \min_{0 \leq k \leq 200} Q(k). \quad (7)$$

Searching for the extremum of the quality function (6), and application of the result for the mirror shift correction is typical for the adaptive process problems. After the mirror translation with the step motor, the operation system searches for the optimum value of the correction voltage, and adapts itself to an unknown situation. Fig. 10 shows the control algorithm.

Collected data of the correction values during the experiment allows building the knowledge base. The base can be used in constructing the expert system.

3.2 Details of the automation – spectrum recognition

The investigations shown above do not give information about a spectral contents of the laser radiation during the laser tuning. Different emission lines are responsible for specific maxima observed at the laser signature – see Figure 5. We elaborated another experimental arrangement to recognize the spectral contents of the laser output gain curve. The arrangement from Figure 6 was rebuilt in a such way, that the detector is allowed moving across the splitted (with the diffraction grating) laser beam – see Figure 11. An algorithm of the procedure is given in Figure 12. The detector can assume a value of its position L_{v_n} in the range from $L_{v_0} = 0$ [mm] to $L_{v_{200}} = L_{v_{\max}} = 20$ [mm] with a resolution of $\Delta L_v = 0.1$ [mm]. An active surface of the detector is 1 mm in diameter, thus moving step is enough to not “loose” any emission line. The range of the investigated frequencies ν depends on the distance of the detector from the diffraction grating.

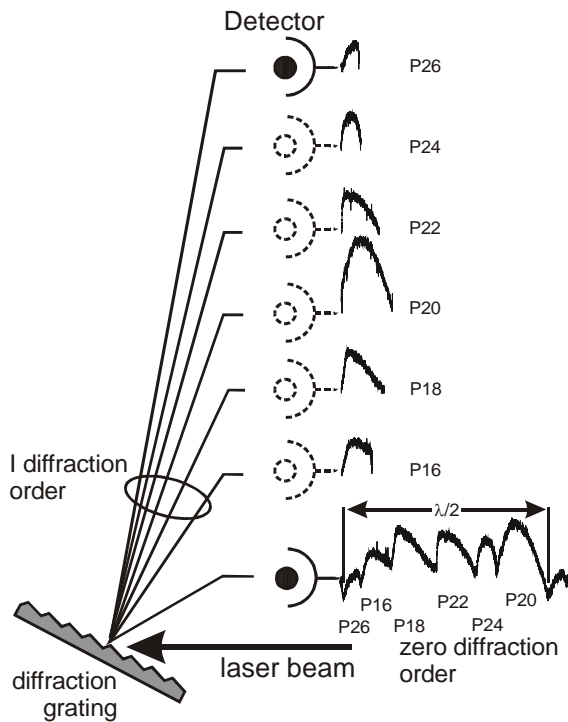


Figure 11: Arrangement for recognizing the spectral contents of the laser output. A moving detector across the splitted (with a diffraction grating) laser beam is used.

Organization of the procedure of the laser spectrum response investigations is similar to the procedure of the calibration given above. This time, additionally, a full procedure of the laser response spectrum scanning is used for each value of a laser resonator length. It means, a detector is moved to next values of the position $L_{v,n}$, and simultaneously a detector output signal U_D is read. The signal depends on both a laser resonator length (a moving indicator is “ l ”, like in the calibration procedure) and detector position (a detector position indicator is “ n ”). It is why a data base read during the experiment is two-dimensional – $U_{D,i,n}$.

The procedure needs calculations of the substitute of the total laser output power for a given length of the laser optical resonator. In the arrangement the detector measures only output laser power for some frequency ranges ν . It is why total laser power, necessary for the calculations, is substituted by sums (8) and (9), which are some approximations of the integration in an integral domain ν .

$$V_{D_j} \cong I = \sum_{n=0}^{200} V_{D_{j,n}}, \quad (8)$$

$$U_{D_j} \cong I = \sum_{n=0}^{200} U_{D_{j,n}}, \quad (9)$$

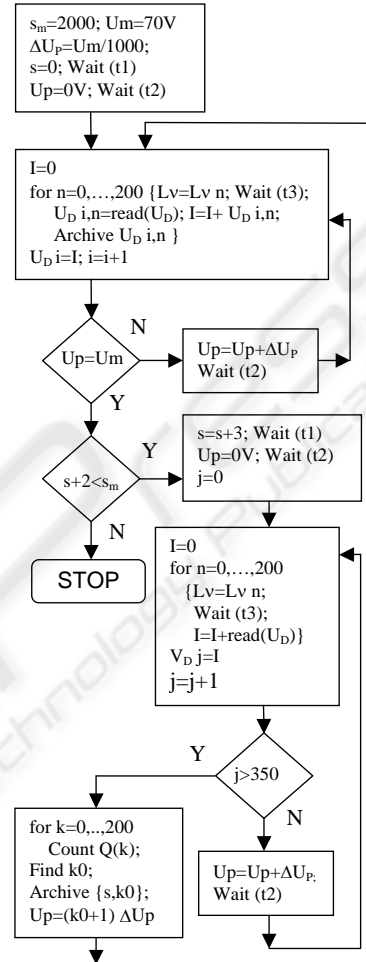


Figure 12: An algorithm used for a spectral recognition of the laser output.

Figure 13 shows an experimental result obtained in the arrangement shown in Figure 11. The observed signature shows a good order, according to an order of the emission lines in the spectrum of a CO_2 molecule. The result is obtained for the laser resonator length of appr. 406 mm. The effect is called a Well-Ordered Laser Signature – WOLS (Plinski², 2000). The signature can be easy calculated, and the result is shown in Figure 13.

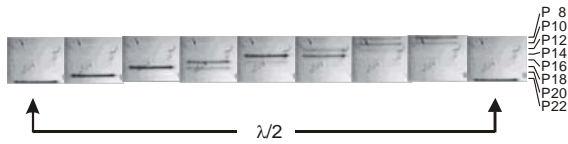


Figure 13: Well-Ordered Laser Signature - experimental result (see the theoretical result in Figure 14 – top)

The result is calculated for the resonator length tuning of many half-lengthwaves $\lambda/2$, to show the developing of the signature with the resonator length change. As seen, the well-ordered signature loses its ordered picture with resonator length changes. In that way it is possible (changing the length of the resonator) to find other signature interesting for many applications.

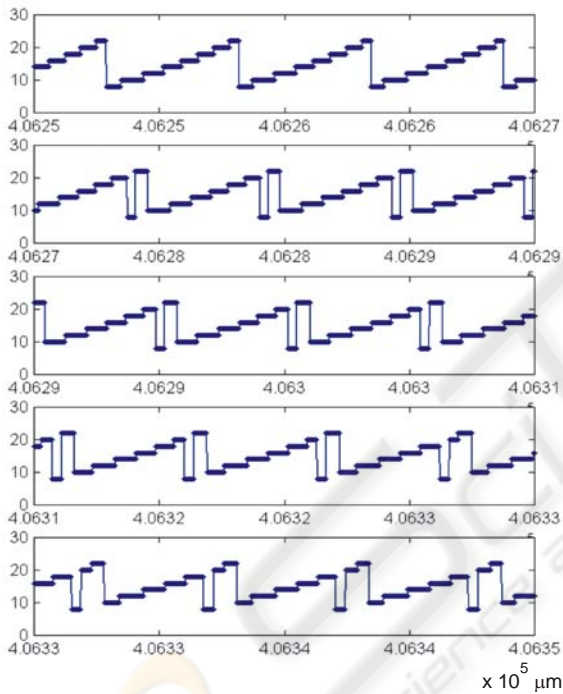


Figure 14: Example of the signatures calculated around of the laser resonator length $L = 406$ mm. Well-ordered laser signature is found (Plinski³, 2000).

One of the applications of the laser is using the laser as a source of a stable radiation. The servo-loop, which stabilize the laser radiation to the centre of the emission line operates much easier, when a passive (temperature) stabilisation is ensured. In this case it is useful to operate on some length of the resonator, where the laser signature is enough “poor”. It means, the line hoppings effect is reduced as much as possible. Figure 15 shows the result obtained around the resonator length of 411.5 mm.

As seen, we observe only one line hopping during the full translation of the laser mirror of $\lambda/2$.

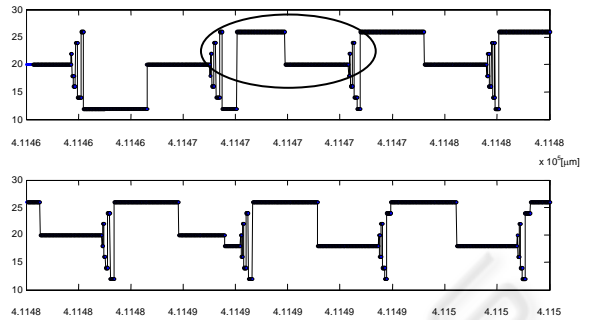


Figure 15: A special case of the signature: an one line jump during the half-wavelength tuning is observed.

To rich the possibility of the elaborated system, it is possible to fill the same mechanical structure of the laser with different gas mixtures of CO₂ containing different isotopes of C an O molecules, as shown in Figure 16.

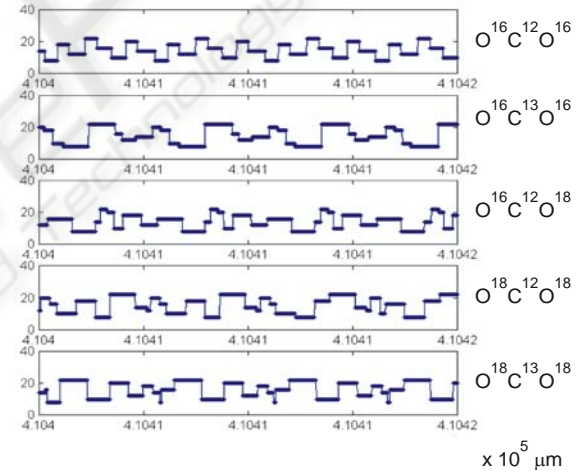


Figure 16: Theoretically calculated laser signatures starting from the length $L = 410.4$ mm of the resonator for different isotopes of carbon and oxygen molecules (data base for the expert system)

As seen, different signatures can be observed for the same length of the resonator.

4 CONCLUSIONS

Our investigations show, that it is possible to find a suitable laser signature for many applications. One of them is a single frequency operation of the laser.

To avoid as much as possible temperature drifts of the laser mirrors we should choose the length of the resonator, where the signature is very poor. It means, the laser operates on one chosen line in a wide range of the resonator tuning.

Another application is a trace gas analyzer. Some gases show a quite narrow dips in the absorption spectrum. Choosing a suitable signature we can tune the laser very easy to desired emission lines, which can be absorbed by investigated gas medium. A good example is a trace analyzer, where the spectral line P14 of the carbon dioxide laser is desired in combinations with P16, or P18, or P20 lines.

The picture of the laser histogram can be easily modified using different isotopes of the carbon or/and oxygen molecules like $O^{16}C^{12}O^{16}$, $O^{16}C^{13}O^{16}$, $O^{16}C^{12}O^{18}$, $O^{18}C^{12}O^{18}$, $O^{18}C^{13}O^{18}$, $O^{16}C^{14}O^{16}$, $O^{18}C^{14}O^{18}$, $O^{16}C^{13}O^{19}$, or $O^{17}C^{12}O^{17}$. Then, different signatures can be observed for the same length of the laser resonator.

Another aspect of the experiment is to create an expert system. As shown, stable and reproducible signatures of the CO₂ laser can be a good standard to calibrate servomechanisms used for investigations of the laser histograms (series of signatures in line). The servomechanism coupled with a given structure of the laser can be applied for investigations of the laser signatures in the large range of the laser tuning independently of the laser medium. The adaptive system to control the laser mirror is used for the corrections of the mirror position errors. The system searches the optimum voltage correction value, to find the optimal position of the laser mirror. The information about the optimum control is collected for each investigated position of the step motor (number of the pitches). Created in that way the data base will be used in further investigations to develop the expert system, which should be helpful for the investigations of the laser histograms of different lasers.

The automation of the described process can help with searching suitable laser signatures for different laser experiments, ex. very sophisticated signatures for some heterodyning experiments (Buholz, 1981), or well-ordered signatures (Plinski², 2000).

The elaborated system for identification of the laser lines can be used as a diffractive mechanism of the laser marker, where the control of the lines generated by a laser is obvious (Plinski⁴, 2000).

Reassuming, a carbon dioxide laser can be designed as a chip spectral device, where choosing a suitable operation frequency can be very easily realized (comparing to expensive, and complicated devices, where one of the laser mirrors is replaced

by a diffraction grating, which stimulates the laser operation on a chosen line).

It is necessary to remark, that the results of the investigations above are possible to obtain rather on the laser in a single-mode operation regime. Then only longitudinal modes are excited in the laser cavity (Siegman, 1986). It is why an unstable resonator is used, which stimulates a single-frequency operation of the laser. In that way, high-order transverse modes (disturbing the picture of the signature) are suppressed by definition.

REFERENCES

- Buholz, N. E., Selected five-color operation of a CO₂ laser. In *Optical Engineering*, Vol. 20, 1981, pp. 325-327.
- Mocker, H. W., Rotational level competition in CO₂ lasers. In *IEEE Journal of Quantum Electronics*, Vol. QE-4, 1968, pp. 769-776.
- Plinski¹, E. F., Witkowski, J. S., Abramski, K. M., Algorithm of RF excited slab-waveguide laser design. In *Journal of Physics D: Applied Physics*, Vol. 33, 2000, pp. 1-4.
- Plinski², E. F., Izvorski, A., Witkowski, J. S., Calibration of an automatic system using a laser signature. In *Journal of Systemics, Cybernetics and Informatics*, Vol. 1, No. 2, 2003 (Ed. *International Institute of Informatics and Systemics*).
- Plinski³, E. F., Witkowski, J. S., Well-ordered laser signature. In *Optics Communications*, Vol. 176, No. 1,2,3, 2000, pp. 207-211.
- Plinski⁴, E. F., Witkowski, J. S., Abramski, K. M., Diffractive mechanism for laser marker. In *Optics and Laser Technology*, Vol. 32, 2000, pp. 33-37.
- Shiffner, G., Prediction of CO₂ laser signatures. In *IEEE Journal of Quantum Electronics*, Vol. QE-8, 1972, pp. 877-881.
- Siegman, A. E., *Lasers*, Mill Valley, University Science Books, California, 1986
- Solnik W., Zajda Z., Automation of oxygenation process in biological treatment plants, in *Datorzinate 2000*, ser. 5, Riga, Rigas Teh. Univ. Zinat. Raksti, 2000, 12-17.
- Waksberg, A. L., Boag, J. C., Sizgoric, S., Signature variations with mirror separation for small sealed CO₂ lasers. In *IEEE Journal of Quantum Electronics*, Vol. QE-7, 1971, pp. 29-35.
- Witteman, W. J., *The CO₂ laser*, Springer Series in Optical Sciences, Berlin, New York, 1987.